Weyl semimetal and topological phase transition in five dimensions

Biao Lian and Shou-Cheng Zhang
Department of Physics, McCullough Building, Stanford University, Stanford, California 94305-4045, USA
(Received 25 February 2017; revised manuscript received 12 May 2017; published 5 June 2017)

We study two Weyl semimetal generalizations in five dimensions (5D) which have Yang monopoles and linked Weyl surfaces in the Brillouin zone, respectively, and carry the second Chern number as a topological number. In particular, we show a Yang monopole naturally reduces to a Hopf link of two Weyl surfaces when the **TP** (time reversal combined with space inversion) symmetry is broken. We then examine the phase transition between insulators with different topological numbers in 5D. In analogy to the three-dimensional case, 5D Weyl semimetals emerge as intermediate phases during the topological phase transition.

DOI: 10.1103/PhysRevB.95.235106

I. INTRODUCTION

The discovery of topological states of matter has greatly enriched the variety of condensed matter in nature [1]. These states usually undergo phase transitions involving a change of topology of the ground-state wave function, which are called topological phase transitions (TPTs). In three dimensions (3D), a significant topological state is the Weyl semimetal [2–5], which plays a key role in TPTs of 3D insulators. An example is the time-reversal-invariant (TRI) transition between a noncentrosymmetric topological insulator (TI) [6,7] and a normal insulator (NI) in 3D, during which an intermediate TRI Weyl semimetal phase inevitably occurs [8,9]. Another example is the TPT between different 3D Chern insulators (CIs) [10], where an intermediate Weyl semimetal phase is also required [11]. In both examples, the topological numbers of the insulators are transferred via Weyl points of the Weyl semimetal phase, which behave as "Dirac monopoles" of the Berry curvature in the Brillouin zone (BZ). The electrons around each Weyl point obey the Weyl equation, with a chirality equal to the first Chern number $C_1 = \pm 1$ of the Berry curvature around the Weyl point.

Recently, there has been a revival of interest in gapless topological phases in higher dimensions, aimed at understanding roles of higher-dimensional topological numbers [7,12–18]. In particular, the Weyl semimetal can be generalized to five dimensions (5D) in two ways: the first is to promote Weyl fermions in 3D to chiral fermions in 5D, which are described by a four-component spinor and have a twofold-degenerate linear energy spectrum. The Dirac monopoles associated with the Weyl points in 3D become the Yang monopoles in 5D [19], which carry a non-Abelian second Chern number $C_2^{NA} = \pm 1$ of the SU(2) Berry curvature of the twofold-degenerate valence (conduction) band [20]. The Yang monopole was first introduced into condensed-matter physics in the construction of the four-dimensional (4D) quantum Hall effect [21]. The second way is to keep the energy spectrum nondegenerate while promoting the Weyl points to linked two-dimensional (2D) Weyl surfaces in the 5D BZ [12,15]. In this case, each Weyl surface carries an Abelian second Chern number $C_2^A \in \mathbb{Z}$ of the U(1) Berry curvature, which is equal to the sum of its linking number with all the other Weyl surfaces [15]. Two natural questions are then whether the two 5D Weyl semimetal generalizations are related and whether they play the role of intermediate phases during the TPT of certain gapped topological states of matter in 5D.

In this paper, we show the two 5D Weyl semimetal generalizations, namely, the Yang monopole and the linked Weyl surfaces in 5D, are closely related via the **TP** symmetry breaking, where **T** and **P** stand for time-reversal and space-inversion, respectively. We then demonstrate they also arise as intermediate phases in the TPT between 5D CI and NI and between 5D TI and NI with particle-hole symmetry **C** that satisfies $\mathbf{C}^2 = -1$ [7,22,23]. In analogy to 3D cases, the Weyl arcs on the boundary of the 5D Weyl semimetal [15] naturally interpolate between the surface states of different gapped topological phases.

II. YANG MONOPOLES AND LINKED WEYL SURFACES

In 3D, a Weyl semimetal is known as a semimetal which is gapless at several points in the BZ, i.e., Weyl points. The low-energy bands near a Weyl point are generically given by a 2×2 Weyl fermion Hamiltonian $H_W(\mathbf{k}) = \sum_{i=1}^{3} v_i(k_i - k_i^W)\sigma^i$ up to an identity term, where $\mathbf{k}$ is the momentum and σ^i $(i = 1,2,3)$ are the Pauli matrices. The Weyl point is located at $\mathbf{k}^W$, while the velocities $v_i \neq 0$ $(i = 1,2,3)$ play the role of light speed. By defining the U(1) Berry connection $a_i(\mathbf{k}) = i\langle u_\mathbf{k}|\partial_{k_i}|u_\mathbf{k}\rangle$ of the valence (conduction) band wave function $|u_\mathbf{k}\rangle$, one can show the first Chern number of the Berry curvature $f_{ij} = \partial_{k_i}a_j - \partial_{k_j}a_i$ on a 2D sphere enclosing $\mathbf{k}^W$ is $C_1 = \mathrm{sgn}(v_1v_2v_3) = \pm 1$, where $\mathrm{sgn}(x)$ is the sign of x. Therefore, the Weyl point $\mathbf{k}^W$ can be viewed as a Dirac monopole of the Berry connection.

The first way to generalize the Weyl semimetal to 5D is to replace the Weyl fermions above by the chiral Dirac fermions in 5D:

$$H_Y(\mathbf{k}) = \sum_{i=1}^{5} v_i\left(k_i - k_i^Y\right)\gamma^i \,, \tag{1}$$

where $\mathbf{k}$ is now the 5D momentum and γ^i $(1 \leqslant i \leqslant 5)$ are the 4×4 gamma matrices satisfying the anticommutation relation $\{\gamma^i, \gamma^j\} = 2\delta^{ij}$. The band structure of such a Hamiltonian is fourfold degenerate at $\mathbf{k}^Y$ and is twofold degenerate everywhere else with a linear dispersion. The twofold degeneracy enables us to define a U(2) Berry connection $a_i^{\alpha\beta}(\mathbf{k}) = i\langle u_\mathbf{k}^\alpha|\partial_{k_i}|u_\mathbf{k}^\beta\rangle$, where $|u_\mathbf{k}^\alpha\rangle$ $(\alpha = 1,2)$ denote the two degenerate wave functions of the valence bands [20]. One can then show the non-Abelian second Chern number C_2^{NA} on a 4D sphere

TABLE I. A Hamiltonian $H(\mathbf{k})$ with $(\mathbf{TP})^2 = +1,0,-1$ is in the real ($\mathbb{R}$), complex ($\mathbb{C}$), and quaternion ($\mathbb{Q}$) classes of the Wigner-Dyson threefold way, respectively, and the Hamiltonians of the 2D Dirac point, 3D Weyl point, and 5D Yang monopole shown here exactly fall into these three classes.

$(\mathbf{TP})^2$	Class	d	Minimal model Hamiltonian
$+1$	$\mathbb{R}$	2	$H(\mathbf{k}) = k_1\sigma^1 + k_2\sigma^3$
0	$\mathbb{C}$	3	$H(\mathbf{k}) = k_1\sigma^1 + k_2\sigma^2 + k_3\sigma^3$
-1	$\mathbb{Q}$	5	$H(\mathbf{k}) = \sum_{i=1}^{5} k_i\gamma^i$

enclosing $\mathbf{k}^Y$ is

$$C_2^{NA} = \oint_{S^4} \frac{d^4\mathbf{k}\epsilon^{ijkl}[\mathrm{tr}(f_{ij}f_{kl}) - (\mathrm{tr}\, f_{ij})(\mathrm{tr}\, f_{kl})]}{32\pi^2} = \pm 1, \quad (2)$$

where $f_{ij} = \partial_{k_i}a_j - \partial_{k_j}a_i - i[a_i,a_j]$ is the non-Abelian U(2) Berry curvature. In this calculation, only the traceless SU(2) part of f_{ij} contributes. Therefore, $\mathbf{k}^Y$ can be viewed as a Yang monopole in the BZ, which is the source of the SU(2) magnetic field in 5D [19]. However, the generic twofold degeneracy of Hamiltonian $H_Y(\mathbf{k})$ requires the system to have certain symmetries. A common symmetry of this kind is the combined **TP** symmetry of time reversal and inversion, which is antiunitary and satisfies $(\mathbf{TP})^2 = -1$ for fermions. Therefore, the Yang monopole 5D generalization is not in the same symmetry class as that of the generic 3D Weyl semimetal.

We remark here that the above 5D Yang monopole, together with the 3D Weyl point and the 2D Dirac point (e.g., in graphene), corresponds exactly to the quaternion (pseudoreal), complex, and real classes of the Wigner-Dyson threefold way [24,25], and the antiunitary **TP** symmetry plays a key role in the classification. Basically, a matrix Hamiltonian $H(\mathbf{k})$ falls into these three classes if $(\mathbf{TP})^2 = -1,0,+1$, respectively (0 stands for no **TP** symmetry), and one can show $d = 5,3,2$ are the corresponding spatial dimensions where pointlike gapless manifolds in the BZ are stable. The minimal Hamiltonians of the three classes are listed in Table I. In particular, $(\mathbf{TP})^2 = +1$ is possible for systems with a negligible spin-orbital coupling such as graphene, where the electrons can be regarded as spinless.

The second 5D Weyl semimetal generalization requires no symmetry (other than the translational symmetry) and thus is in the same symmetry class as the 3D Weyl semimetal. Its band structure is nondegenerate except for a few closed submanifolds $\mathcal{M}_j$ called Weyl surfaces, where two bands cross each other [15]. The effective Hamiltonian near each $\mathcal{M}_j$ involves only the two crossing bands and takes the 2×2 form $H_W(\mathbf{k}) = \xi_0(\mathbf{k}) + \sum_{i=1}^{3}\xi_i(\mathbf{k})\sigma^i$. Therefore, $\mathcal{M}_j$ is locally determined by three conditions $\xi_i(\mathbf{k}) = 0$ $(i = 1,2,3)$. In one band α of the two associated with $\mathcal{M}_j$, one can define a U(1) Berry connection $a_i^{(\alpha)}(\mathbf{k}) = i\langle u_{\mathbf{k}}^{\alpha}|\partial_{k_i}|u_{\mathbf{k}}^{\alpha}\rangle$ with its wave function $|u_{\mathbf{k}}^{\alpha}\rangle$ and define the U(1) second Chern number of $\mathcal{M}_j$ in band α on a 4D closed manifold $\mathcal{V}$ that encloses only $\mathcal{M}_j$ as

$$C_2^A(\mathcal{M}_j,\alpha) = \oint_{\mathcal{V}} \frac{d^4\mathbf{k}\epsilon^{ijkl} f_{ij}^{(\alpha)} f_{kl}^{(\alpha)}}{32\pi^2} \in \mathbb{Z}, \quad (3)$$

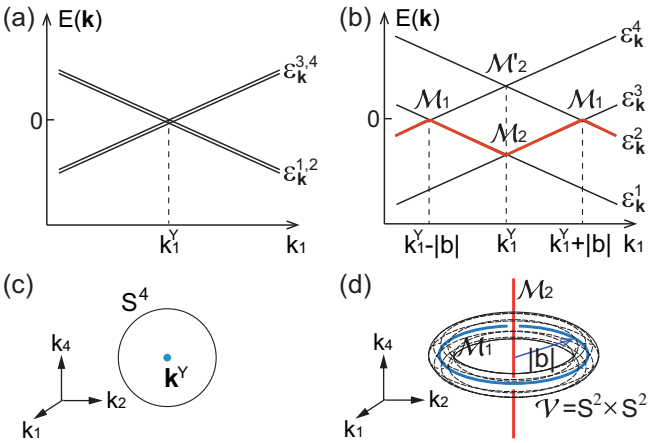

FIG. 1. (a) Doubly degenerate band structure near a Yang monopole plotted at $\tilde{k}_i = 0$ $(2 \leqslant i \leqslant 5)$. (b) The band structure and Weyl surfaces in the presence of the **TP**-breaking b term. (c) Yang monopole enclosed by S^4 shown in the 3D subspace $\tilde{k}_3 = \tilde{k}_5 = 0$. (d) The Hopf link of Weyl surfaces $\mathcal{M}_1$ and $\mathcal{M}_2$ shown in 3D subspace $\tilde{k}_3 = \tilde{k}_5 = 0$ (thick red and blue lines) and a 4D manifold $\mathcal{V} = S^2 \times S^2$ enclosing Weyl surface $\mathcal{M}_1$ (appearing as a torus).

where $f_{ij}^{(\alpha)}$ is the Berry curvature of $a_i^{(\alpha)}$. Remarkably, we showed in an earlier paper that [15]

$$C_2^A(\mathcal{M}_j,\alpha) = \sum_{\ell\in\alpha,\ell\neq j} \Phi(\mathcal{M}_j,\mathcal{M}_\ell), \quad (4)$$

where $\Phi(\mathcal{M}_j,\mathcal{M}_\ell)$ is the linking number between $\mathcal{M}_j$ and $\mathcal{M}_\ell$ in the 5D BZ and $\mathcal{M}_\ell$ runs over all the Weyl surfaces associated with band α.

The relation between the above two 5D generalizations can be most easily seen in the following four-band model with Hamiltonian

$$H'_Y(\mathbf{k}) = \sum_{i=1}^{5}(k_i - k_i^Y)\gamma^i + b\frac{i[\gamma^4,\gamma^5]}{2}, \quad (5)$$

where b is a real parameter that breaks the **TP** symmetry. When $b = 0$, the Hamiltonian reduces to the Yang monopole Hamiltonian $H_Y(\mathbf{k})$ in Eq. (1), where we have set all the velocities to $v_i = 1$. When $b \neq 0$, the **TP** symmetry is broken, and the Yang monopole necessarily evolves into linked Weyl surfaces. This can be seen explicitly by deriving the energy spectrum $\epsilon_{\mathbf{k}}^{\alpha} = \pm\{[(\tilde{k}_1^2 + \tilde{k}_2^2 + \tilde{k}_3^2)^{1/2} \pm b]^2 + \tilde{k}_4^2 + \tilde{k}_5^2\}^{1/2}$, where we have defined $\tilde{k}_i = k_i - k_i^Y$ $(1 \leqslant i \leqslant 5)$. Here $1 \leqslant \alpha \leqslant 4$ denotes the αth band in energies. Figures 1(a) and 1(b) show the band structures for $b = 0$ and $b \neq 0$, respectively, where $\tilde{k}_2,\tilde{k}_3,\tilde{k}_4,\tilde{k}_5$ are assumed to be zero. In the $b \neq 0$ case, one can readily identify three Weyl surfaces: $\mathcal{M}_1$ between bands $\epsilon_{\mathbf{k}}^2$ and $\epsilon_{\mathbf{k}}^3$, $\mathcal{M}_2$ between bands $\epsilon_{\mathbf{k}}^1$ and $\epsilon_{\mathbf{k}}^2$, and $\mathcal{M}'_2$ between bands $\epsilon_{\mathbf{k}}^3$ and $\epsilon_{\mathbf{k}}^4$ [see Fig. 1(b)]. $\mathcal{M}_1$ is a 2D sphere given by $\tilde{k}_1^2 + \tilde{k}_2^2 + \tilde{k}_3^2 = b^2$ and $\tilde{k}_4 = \tilde{k}_5 = 0$, while $\mathcal{M}_2$ and $\mathcal{M}'_2$ coincide and are a 2D plane given by $\tilde{k}_1 = \tilde{k}_2 = \tilde{k}_3 = 0$. In particular, the second band $\epsilon_{\mathbf{k}}^2$ [thick red line in Fig. 1(b)] is associated with $\mathcal{M}_1$ and $\mathcal{M}_2$, which form a Hopf link in 5D, as can be seen in the 3D subspace $k_3 = k_5 = 0$ plotted in Fig. 1(d). In the limit $b \to 0$, the radius of $\mathcal{M}_1$ contracts to zero, so $\mathcal{M}_1$ collapses onto $\mathcal{M}_2$ (and $\mathcal{M}'_2$) and becomes

the fourfold-degenerate Yang monopole in Fig. 1(c). One can add other small **TP**-breaking terms to Eq. (5), and the above picture remains topologically unchanged.

Due to the **TP** symmetry breaking, the U(2) gauge field $a_i(\mathbf{k})$ is broken down to two U(1) gauge fields, $a_i^{(1)}(\mathbf{k})$ and $a_i^{(2)}(\mathbf{k})$, in bands $\epsilon_{\mathbf{k}}^1$ and $\epsilon_{\mathbf{k}}^2$. One can easily check the Abelian second Chern number of $\mathcal{M}_1$ calculated from $a_i^{(2)}(\mathbf{k})$ is $C_2^A(\mathcal{M}_1,2)=1$, which is defined on the 4D manifold $\mathcal{V}$ with topology $S^2\times S^2$, as shown in Fig. 1(d) [15]. This is closely related to the non-Abelian second Chern number $C_2^{NA}=1$ of the Yang monopole before symmetry breaking. In fact, ignoring the gauge invariance, we can still define the U(2) gauge field $a_i^{\alpha\beta}(\mathbf{k})$ using the two valence bands of Hamiltonian $H_Y'(\mathbf{k})$, which is singular on $\mathcal{M}_1$ but not on $\mathcal{M}_2$ [since $\mathcal{M}_2$ is between the two bands defining the U(2) Berry connection] and still satisfies $C_2^{NA}=1$ on a sphere S^4 enclosing $\mathcal{M}_1$. The sphere S^4 can be deformed adiabatically into $\mathcal{V}$ in Fig. 1(d), so we also have $C_2^{NA}=1$ on $\mathcal{V}$. To see C_2^{NA} is equal to $C_2^A(\mathcal{M}_1,2)$, we can take the limit where $\mathcal{V}$ is a thin "torus" $S^2\times S^2$; that is, its smaller radius (distance to $\mathcal{M}_1$) tends to zero. In this limit, one will find $\int_{\mathcal{V}} d^4\mathbf{k}\epsilon^{ijkl}f_{ij}^{12}f_{kl}^{21}=0$; namely, the off-diagonal elements of field strength f_{ij} do not contribute (see Appendix A). So C_2^{NA} is given solely by the diagonal field strengths f_{ij}^{11} and f_{ij}^{22}, which can be roughly identified with U(1) Berry curvatures of bands 1 and 2. By calculations, one can show $\epsilon^{ijkl}f_{ij}^{11}f_{kl}^{11}=\epsilon^{ijkl}\mathrm{tr}\,f_{ij}\mathrm{tr}\,f_{kl}=0$. A heuristic understanding of this is the Berry curvature f_{ij}^{11} of band 1 sees only $\mathcal{M}_2$, while the U(1) trace Berry curvature $\mathrm{tr}\,f_{ij}$ sees only $\mathcal{M}_1$, so both of them do not see linked Weyl surfaces and have zero contribution to the second Chern number. One can then readily show $C_2^{NA}=\int_{\mathcal{V}} d^4\mathbf{k}\epsilon^{ijkl}f_{ij}^{22}f_{kl}^{22}/32\pi^2=\int_{\mathcal{V}} d^4\mathbf{k}\epsilon^{ijkl}f_{ij}^{(2)}f_{kl}^{(2)}/32\pi^2=C_2^A(2,\mathcal{M}_1)$. We note that in this limit where $\mathcal{V}$ is closely attached to $\mathcal{M}_1$, only the diagonal elements of f_{ij} contribute, while in the Yang monopole case which is spherically symmetric, the diagonal and off-diagonal elements are equally important [19].

In high-energy physics, a U(2) gauge symmetry can be spontaneously broken down to U(1) × U(1) via the Georgi-Glashow mechanism [26] with an isospin-1 Higgs field. In 5D space, SU(2) gauge fields are associated with pointlike Yang monopoles, while U(1) gauge fields are associated with monopole 2-branes (codimension-3 objects). We conjecture that a gauge symmetry breaking from U(2) to U(1) × U(1) in 5D will always break an SU(2) Yang monopole into two linked U(1) monopole 2-branes $\mathcal{M}_1$ and $\mathcal{M}_2$, where $\mathcal{M}_1$ is coupled to one of the two U(1) gauge fields, while $\mathcal{M}_2$ is coupled to both U(1) gauge fields with opposite monopole charges.

III. TOPOLOGICAL PHASE TRANSITIONS IN 5D

It is known that 3D Weyl semimetals play an important role in 3D TPTs. An example is the TPT of the 3D CI with no symmetry, which is characterized by three integers (n_1,n_2,n_3), with n_i being the first Chern number in the plane orthogonal to k_i in the BZ [10,11]. The CI becomes a NI when all $n_i=0$. The TPT from a 3D NI to a (0,0,1) CI involves an intermediate Weyl semimetal phase, as shown in Figs. 2(a)–2(c). By creating a pair of Weyl points with opposite monopole charges and annihilating them after winding along a closed cycle in the k_3 direction, one creates Berry flux quanta in the k_1-k_2 plane, and n_3 increases by 1 [11]. At the same time, a Fermi arc arises on the real-space boundary connecting the projections of the two Weyl points [4], which finally becomes a closed Fermi loop along k_3. Another example is the TPT from TI to NI, which are the two phases in the $\mathbb{Z}_2$ classification of 3D TRI insulators [6,7]. When the inversion symmetry is broken, an intermediate TRI Weyl semimetal arises [8,9], which contains (multiples of) four Weyl points, as shown in Figs. 2(d)–2(f). The TPT is done by creating two pairs of Weyl points with opposite charges, winding them along a loop that encloses a TRI point (e.g., Γ point), then annihilating them in pairs with their partners exchanged. Meanwhile, the Fermi surface loop of the Dirac surface states of TI breaks into two Fermi arcs connecting the four Weyl points, which vanish when all the Weyl points are gone.

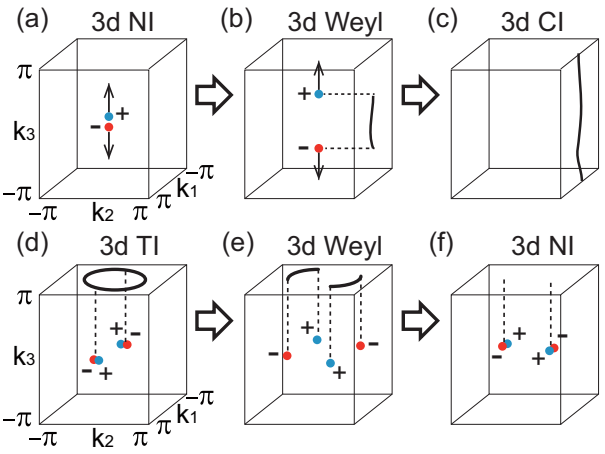

FIG. 2. (a)–(c) TPT from a 3D NI to a 3D CI via creation and annihilation of a pair of Weyl points in the BZ. (d)–(f) TPT from a 3D TI to a 3D NI, which involves winding of (multiples of) four Weyl points.

Similarly, the 5D TPTs involve creation of 5D Weyl semimetal phases. We first examine the TPT of 5D CIs with no symmetry, which are characterized by five second Chern numbers n_i in the 4D hyperplanes of the BZ orthogonal to k_i $(1\leqslant i\leqslant 5)$ and ten first Chern numbers n_{ij} in the 2D planes parallel to k_i and k_j $(1\leqslant i<j\leqslant 5)$. The second Chern numbers n_i are even under both **T** and **P** transformations, while the first Chern numbers n_{ij} are odd under **T** and even under **P**. Here we shall show that changes of the five n_i will involve creation and annihilation of linked Weyl surfaces in the BZ. A simple example without **TP** symmetry is the following four-band Hamiltonian:

$$H_{QH}(\mathbf{k})=\sum_{i=1}^{5}\xi_i(\mathbf{k})\gamma^i+b\frac{i[\gamma^3,\gamma^4]}{2}, \tag{6}$$

where $\xi_i(\mathbf{k})=\sin k_i$ for $1\leqslant i\leqslant 4$ and $\xi_5(\mathbf{k})=m+\sum_{i=1}^{4}(1-\cos k_i)+\eta(1-\cos k_5)$. Here m is a tuning parameter, while $0\leqslant b<\eta<1-b$. We shall label each band by its order in energies and assume the lower two bands are occupied. Through an analysis similar to what we did following Eq. (5), the Weyl surfaces between bands 2 and 3 are given by $\xi_1^2+\xi_2^2+\xi_5^2=b^2$ and $\xi_3=\xi_4=0$, while

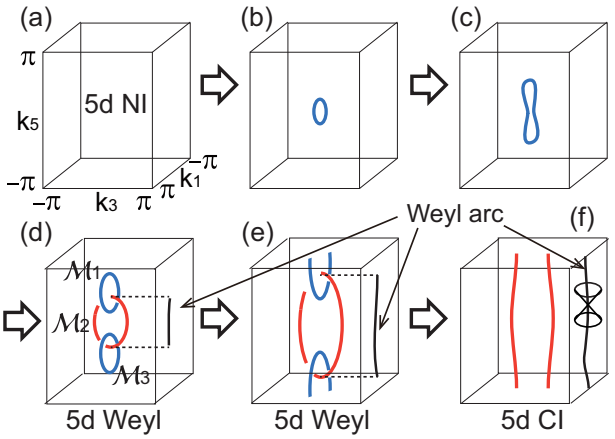

FIG. 3. The evolution of Weyl surfaces in the 5D TPT from NI to CI, plotted in 3D subspace $k_2 = k_4 = 0$. The blue loops are Weyl surfaces between bands 2 and 3, while the red loop is that between bands 1 and 2.

those between bands 1 and 2 (also 3 and 4) are given by $\xi_1 = \xi_2 = \xi_5 = 0$. These two kinds of Weyl surfaces are drawn as blue and red in the 3D subspace $k_2 = k_4 = 0$ of the BZ shown in Fig. 3, respectively, where they appear as one-dimensional loops.

When $m > b$, the system is a 5D NI with all n_i and n_{ij} zero and no Weyl surfaces [Fig. 3(a)]. The TPT to a 5D CI with $n_5 = 1$ is driven by decreasing m, which experiences the following stages: when $-b < m < b$, a Weyl surface between bands 2 and 3 arises around the origin, which is topologically a 2D sphere in the $k_3 = k_4 = 0$ hyperplane [Figs. 3(b) and 3(c)]. When $b - 2\eta < m < -b$, as shown in Fig. 3(d), the 2D sphere between bands 2 and 3 splits into two smaller spheres $\mathcal{M}_1$ and $\mathcal{M}_3$ (blue) in the $k_3 = k_4 = 0$ hyperplane, while another 2D sphere Weyl surface $\mathcal{M}_2$ (red) between bands 1 and 2 is created in the $k_1 = k_2 = 0$ plane, which is linked to both $\mathcal{M}_1$ and $\mathcal{M}_3$. As m is further decreased, $\mathcal{M}_1$ and $\mathcal{M}_3$ will move along $\pm k_5$, respectively, and finally merge into a single Weyl surface when $-b - 2\eta < m < b - 2\eta$ [Fig. 3(e)]. This Weyl surface then shrinks to zero, and the system becomes a 5D CI with $n_5 = 1$ for $b - 2 < m < -b - 2\eta$, leaving a cylindrical Weyl surface $\mathcal{M}_2$ between bands 1 and 2 [and also one between bands 3 and 4, Fig. 3(f)]. We note that if $b = 0$, the **TP** symmetry is restored, and the two blue Weyl surfaces $\mathcal{M}_1$ and $\mathcal{M}_3$ will collapse into two Yang monopoles of opposite monopole charges C_2^{NA}. The TPT process then becomes the creation, winding, and annihilation of two Yang monopoles.

This TPT is also accompanied by a surface-state evolution from trivial to nontrivial. It has been shown [15] that a 5D Weyl semimetal with linked Weyl surfaces contains protected Weyl arcs in the 4D momentum space of surface states, which have linear dispersions in the other three directions perpendicular to the arc. By taking an open boundary condition along the k_3 direction, one can obtain a Weyl arc on the 4D boundary connecting the projections of the two Weyl surface Hopf links [Figs. 3(d) and 3(e)]. When the system becomes a CI, the Weyl arc develops into a noncontractible Weyl loop along k_5 as expected.

The second example is the TPT between **TP**-breaking 5D insulators with particle-hole symmetry **C** satisfying $\mathbf{C}^2 = -1$, which are shown to be classified by $\mathbb{Z}_2$ into 5D TIs and NIs [7,22,23]. Here we consider an eight-band model Hamiltonian of a 5D TI as follows:

$$H_{\mathrm{TI}}(\mathbf{k}) = \sum_{i=1}^{6} \zeta_i(\mathbf{k})\Gamma^i + H_A, \tag{7}$$

where Γ^i $(1 \leqslant i \leqslant 7)$ are the 8×8 gamma matrices chosen so that Γ^1, Γ^2, Γ^3, and Γ^7 are real and Γ^4, Γ^5, and Γ^6 are imaginary, $\zeta_i(\mathbf{k}) = \sin k_i$ for $1 \leqslant i \leqslant 5$, $\zeta_6(\mathbf{k}) = m + \sum_{i=1}^{5} t_i(1 - \cos k_i)$ with $t_i > 0$, and

$$H_A = i\eta_0\Gamma^1\Gamma^2\Gamma^7 + \eta_1\Gamma^7 \sin k_5 + i\eta_2\Gamma^3\Gamma^4\Gamma^5 + i\eta_3\Gamma^3\Gamma^4 \tag{8}$$

is a symmetry-breaking perturbation. The **T**, **P**, and **C** transformation matrices are given by $\mathcal{T} = \Gamma^4\Gamma^5\Gamma^7$, $\mathcal{P} = i\Gamma^6$, and $\mathcal{C} = \Gamma^4\Gamma^5$, and a Hamiltonian $H(\mathbf{k})$ will have these symmetries if $\mathcal{T}^\dagger H(-\mathbf{k})\mathcal{T} = H^*(\mathbf{k})$, $\mathcal{P}^\dagger H(-\mathbf{k})\mathcal{P} = H(\mathbf{k})$, and $\mathcal{C}^\dagger H(-\mathbf{k})\mathcal{C} = -H^*(\mathbf{k})$, respectively. It is then easy to see that H_A respects the **C** symmetry but breaks **T**, **P**, and **TP** symmetries. In particular, only η_1 and η_2 break the **TP** symmetry.

In the absence of H_A, the system is a 5D NI if $m > 0$ and is a 5D TI if $m < 0$. With the symmetry-breaking term H_A, the calculation of the band structure of $H_{\mathrm{TI}}(\mathbf{k})$ becomes more complicated. For simplicity, we shall examine only the limiting case where $(t_1/t_2)^2 + \eta_0^2 < 1$, $|\eta_0| \gg |\eta_1|$, $|\eta_0| \gg |\eta_2|$, and $|\eta_0\eta_1| \gg |\eta_3|$ [with t_1 and t_2 as defined in the expression for $\zeta_6(\mathbf{k})$]. We shall label each band by its order in energies and keep the Fermi energy at zero, i.e., between bands 4 and 5, as required by the **C** symmetry. To a good approximation, the Weyl surfaces between bands 4 and 5 are given by $\zeta_1^2 + \zeta_2^2 = \eta_0^2$, $\zeta_3^2 + \zeta_4^2 + \zeta_5^2 = \eta_2^2$, and $\zeta_6 = 0$, while those between bands 5 and 6 (and also between 3 and 4) are given by $\zeta_3 = \zeta_4 = \zeta_5 = 0$. The TPT can be driven by tuning m from negative (TI) to positive (NI), and the evolution of these low-energy Weyl surfaces is illustrated in Figs. 4(a)–4(f) in the 3D subspace $k_1^2 + k_2^2 = \eta_0^2$ and $k_4 = 0$. The small blue loops are the images of Weyl surfaces between bands 4 and 5, while the red loop at $k_3 = k_5 = 0$ is that between bands 5 and 6. At first, two pairs of blue Weyl surfaces arise unlinked [Fig. 4(b)]. As m increases, they merge into four new Weyl surfaces linked with the red Weyl surface, which then wind around the red Weyl surface and merge into unlinked pairs again with their partners exchanged [Figs. 4(c)–4(e)]. Finally, the four unlinked blue Weyl surfaces contract to zero, and the system becomes a 5D NI. Similar to the CI case, if $\eta_1 = \eta_2 = 0$, the **TP** symmetry is recovered, and the four blue Weyl surfaces will collapse into four Yang monopoles. The TPT process then involves the winding of Yang monopoles instead of linked Weyl surfaces. The topological surface states of the system also involve a topological transition during the TPT. The topological surface states of a noncentrosymmetric 5D TI are generically a "Weyl ring," as shown in Fig. 4(g). The TPT then breaks into two Weyl arcs [Fig. 4(h)], which finally vanish when entering the NI phase.

In conclusion, we showed that 5D Weyl semimetals with Yang monopoles are protected by the **TP** symmetry and

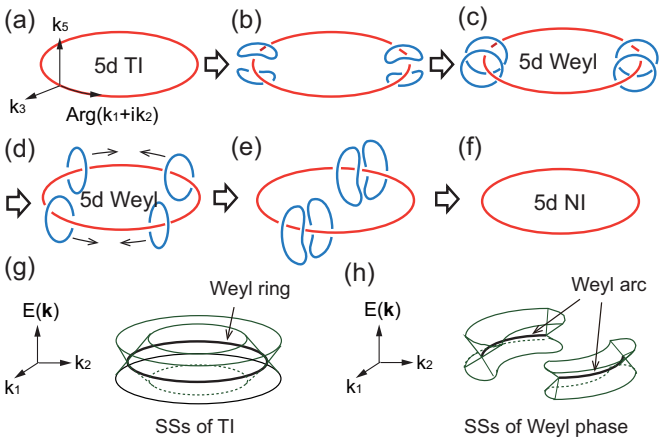

FIG. 4. (a)–(f) The TPT from 5D TI to NI shown in 3D subspace $k_1^2+k_2^2=\eta_0^2$ and $k_4=0$. The small blue loops are the Weyl surfaces at the Fermi energy between bands 4 and 5, while the large red loop is that between bands 3 and 4. (g) and (h) The evolution of surface states from a Weyl ring to two Weyl arcs during the TPT.

generically reduce to 5D Weyl semimetals with linked Weyl surfaces in the presence of **TP** symmetry breaking. We therefore expect that Yang monopoles generically break into linked U(1) monopole 2-branes in 5D theories of gauge symmetry breaking from U(2) to U(1) × U(1). As gapless states carrying the second Chern number, they emerge as intermediate phases in the TPTs between CIs and NIs or between TIs and NIs in 5D space, generalizing the connection between gapless and gapped topological phases in 3D [8,9].

ACKNOWLEDGMENTS

We would like to thank J.-Y. Chen for helpful discussions during the research. This work is supported by the NSF under Grant No. DMR-1305677.

APPENDIX A: DERIVATION OF $C_2^{NA}=C_2^A(\mathcal{M}_1,2)$ ON MANIFOLD $\mathcal{V}$

It is sufficient to do the calculation in the limit where $\mathcal{V}$ is thin, i.e., close to Weyl surface $\mathcal{M}_1$. For the model given in Eq. (5), such a 4D manifold $\mathcal{V}$ can be given by $(\kappa-b)^2+\tilde{k}_4^2+\tilde{k}_5^2=\epsilon^2$, where $\kappa=\sqrt{\tilde{k}_1^2+\tilde{k}_2^2+\tilde{k}_3^2}$ and $\epsilon\ll b$. Using Γ matrices defined in [15], the wave function $|u_{\mathbf{k}}^2\rangle$ is given by

$$|u_{\mathbf{k}}^2\rangle=\Big(\cos\frac{\theta}{2}\cos\frac{\alpha}{2},\sin\frac{\theta}{2}\cos\frac{\alpha}{2}e^{i\phi},\times\cos\frac{\theta}{2}\sin\frac{\alpha}{2}e^{i\psi},\sin\frac{\theta}{2}\cos\frac{\alpha}{2}e^{i\phi+i\psi}\Big),\quad\text{(A1)}$$

while $|u_{\mathbf{k}}^1\rangle$ is well approximated by

$$|u_{\mathbf{k}}^1\rangle=\Big(\sin\frac{\theta}{2},-\cos\frac{\theta}{2}e^{i\phi},0,0\Big),\quad\text{(A2)}$$

where we have defined the angles α,ψ,θ,ϕ by $\sin\alpha e^{i\psi}=(k_4+ik_5)/\epsilon$ and $\sin\theta e^{i\phi}=(k_1+ik_2)/\kappa$. This approximation basically ignores the dependence of $|u_{\mathbf{k}}^1\rangle$ on k_4 and k_5, which is valid since $|\tilde{k}_{4,5}|<\epsilon\ll b$ and $|u_{\mathbf{k}}^1\rangle$ is nonsingular at $\mathcal{M}_1$.

The nonzero components of the U(2) Berry connection $a_{\mathbf{k}}^{\alpha\beta}$ can then be shown to be

$$a_\phi^{11}=-\frac{1+\cos\theta}{2},\quad a_\phi^{22}=-\frac{1-\cos\theta}{2},$$
$$a_\psi^{22}=-\frac{1-\cos\alpha}{2},\quad a_\theta^{21}=\frac{i}{2}\cos\theta\cos\frac{\alpha}{2},$$
$$a_\phi^{21}=\frac{1}{2}\sin\theta\cos\frac{\alpha}{2},\quad\text{(A3)}$$

with $a_i^{12}=a_i^{21*}$. It is then straightforward to calculate the non-Abelian field strengths $f_{ij}^{\alpha\beta}$. In particular, one can prove that $\epsilon^{ijkl}f_{ij}^{12}f_{kl}^{21}=[\sin2\theta(1-\cos\alpha)\sin\alpha]/8$, which gives zero when integrated over the four angles. Therefore, the off-diagonal components of f_{ij} have no contribution to the second Chern number C_2^{NA}. Further, one can show $f_{\theta\phi}^{22}=-f_{\theta\phi}^{11}=f_{\theta\phi}^{(2)}+(\sin2\theta\cos\alpha)/4$ and $f_{\alpha\psi}^{22}=f_{\alpha\psi}^{(2)}=(\sin\alpha)/2$ are the only rest nonzero terms, where $f_{ij}^{(1)}$ and $f_{ij}^{(2)}$ are the U(1) Berry connection in bands 1 and 2, respectively. Therefore, we have $\epsilon^{ijkl}f_{ij}^{11}f_{kl}^{11}=\epsilon^{ijkl}\mathrm{tr}f_{ij}\mathrm{tr}f_{kl}=0$ and $\epsilon^{ijkl}f_{ij}^{22}f_{kl}^{22}=\epsilon^{ijkl}f_{ij}^{(2)}f_{kl}^{(2)}+\sin2\theta\sin2\alpha$. The non-Abelian second Chern number is then

$$C_2^{NA}=\int_0^\pi d\theta\int_0^{2\pi}d\phi\int_0^\pi d\alpha\int_0^{2\pi}d\psi\frac{\epsilon^{ijkl}f_{ij}^{22}f_{kl}^{22}}{32\pi^2}=\oint_{\mathcal{V}}\frac{d^4\mathbf{k}\epsilon^{ijkl}f_{ij}^{(2)}f_{kl}^{(2)}}{32\pi^2}=C_2^A(2,\mathcal{M}_1)=1.\quad\text{(A4)}$$

If we rewrite the non-Abelian field strength as $f_{ij}=f_{ij}^at^a$, where $t^a=(1,\sigma^1,\sigma^2,\sigma^3)/2$ $(a=0,1,2,3)$ are the generators of U(2), the non-Abelian second Chern number on $\mathcal{V}$ can be expressed as

$$C_2^{NA}=-c^0+c^1+c^2+c^3,$$

where we have defined $c^a=\int_{\mathcal{V}}d^4\mathbf{k}\epsilon^{ijkl}f_{ij}^af_{kl}^a/64\pi^2$. In the limit where $\mathcal{V}$ is close to $\mathcal{M}_1$, the above calculations tell us that $c_0=c_1=c_2=0$ and $c_3=C_2(2,\mathcal{M}_1)=1$. In contrast, in the Yang monopole case, which is rotationally symmetric, one can show $c_0=0$ and $c_1=c_2=c_3=1/3$. Therefore, the TP symmetry breaking also breaks the symmetry between c_1, c_2, and c_3.

APPENDIX B: WEYL SURFACES OF MODEL HAMILTONIAN (7)

Compared to the four-band model in Eq. (6) which can be easily diagonalized, the eight-band model $H_{\mathrm{TI}}(\mathbf{k})$ in Eq. (7) has a band structure more difficult to calculate. Here we present an easier way to examine the band structure with the assumptions $(t_1/t_2)^2+\eta_0^2<1$, $|\eta_0|\gg|\eta_1|,|\eta_0|\gg|\eta_2|$, and $|\eta_0\eta_1|\gg|\eta_3|$.

For the moment we shall assume $\eta_3=0$. To solve the Schrödinger equation $H_{\mathrm{TI}}|\psi\rangle=E|\psi\rangle$, one can first rewrite it as $H_{\mathrm{TI}}^2|\psi\rangle=E^2|\psi\rangle$, which reduces to

$$\Big(E^2-\sum_{i=1}^6\xi_i^2-\eta_0^2-\eta_1^2\sin^2k_5-\eta_2^2\Big)|\psi\rangle=(\Lambda_0+\Lambda_2)|\psi\rangle\quad\text{(B1)}$$

after making use of the properties of Γ matrices, where we have defined

$$\Lambda_0 = 2\eta_0(\zeta_1\Gamma^2\Gamma^7 - \zeta_2\Gamma^1\Gamma^7 + \eta_1 \sin k_5\Gamma^1\Gamma^2),$$
$$\Lambda_2 = 2\eta_2(\zeta_3\Gamma^4\Gamma^5 - \zeta_4\Gamma^3\Gamma^5 + \zeta_5\Gamma^3\Gamma^4).$$

One can easily show that $\Lambda_0^2 = 4\eta_0^2(\zeta_1^2 + \zeta_2^2 + \eta_1^2 \sin^2 k_5) = \eta_0^2\chi_0^2$, $\Lambda_2^2 = 4\eta_2^2(\zeta_3^2 + \zeta_4^2 + \zeta_5^2) = \eta_2^2\chi_2^2$, and $[\Lambda_0, \Lambda_2] = 0$. Therefore, Γ_0 and Γ_2 can be simultaneously diagonalized, i.e., $\Lambda_0 = \pm\eta_0\chi_0$, $\Lambda_2 = \pm\eta_2\chi_2$. One then obtains the energy spectrum of the eight bands as

$$E = \pm\sqrt{(\eta_0 \pm \chi_0)^2 + (\eta_2 \pm \chi_2)^2 + \zeta_6^2}. \tag{B2}$$

One can then see the Weyl surfaces between bands 4 and 5 are given by $\chi_0^2 = \zeta_1^2 + \zeta_2^2 + \eta_1^2 \sin^2 k_5 = \eta_0^2$, $\chi_2^2 = \zeta_3^2 + \zeta_4^2 + \zeta_5^2 = \eta_2^2$, and $\zeta_6 = 0$. Since $|\eta_0| \gg |\eta_1|$, one can approximately ignore the $\eta_1^2 \sin^2 k_5$ term.

It is also easy to see that the Weyl surfaces between bands 3 and 4 are given by $\chi_2 = 0$, i.e., $\zeta_3 = \zeta_4 = \zeta_5 = 0$, which is exactly the k_1-k_2 plane. However, another set of Weyl surfaces is given by $\chi_0 = 0$, i.e., $\zeta_1 = \zeta_2 = \sin k_5 = 0$, which gives the k_3-k_4 plane in touch with the above Weyl surface (the k_1-k_2 plane). Such a configuration is unstable against perturbations in 5D.

This touching of Weyl surfaces is removed when one adds the η_3 term. Via a perturbation analysis, one can show the η_3 term splits the above two kinds of Weyl surfaces in the k_5 direction for a distance of about order $|\eta_3 E/\eta_0\eta_1|$ away.

The Weyl surfaces between bands 4 and 5 and between bands 5 and 6 can then be plotted according to the expression of the functions ζ_i, which are as illustrated in Fig. 4. In particular, the condition $(t_1/t_2)^2 + \eta_0^2 < 1$ limits the number of Weyl surfaces between bands 4 and 5 to only four.

[1] X.-L. Qi and S.-C. Zhang, Rev. Mod. Phys. **83**, 1057 (2011).
[2] M. V. Berry, Proc. R. Soc. London, Ser. A **392**, 45 (1984).
[3] H. Nielsen and M. Ninomiya, Phys. Lett. B **130**, 389 (1983).
[4] X. Wan, A. M. Turner, A. Vishwanath, and S. Y. Savrasov, Phys. Rev. B **83**, 205101 (2011).
[5] L. Balents, Physics **4**, 36 (2011).
[6] L. Fu, C. L. Kane, and E. J. Mele, Phys. Rev. Lett. **98**, 106803 (2007).
[7] X.-L. Qi, T. L. Hughes, and S.-C. Zhang, Phys. Rev. B **78**, 195424 (2008).
[8] S. Murakami, New J. Phys. **9**, 356 (2007).
[9] S. Murakami, M. Hirayama, R. Okugawa, and T. Miyake, Sci. Adv. **3**, e1602680 (2017).
[10] M. Kohmoto, B. I. Halperin, and Y.-S. Wu, Phys. Rev. B **45**, 13488 (1992).
[11] F. D. M. Haldane, Phys. Rev. Lett. **93**, 206602 (2004).
[12] P. Hořava, Phys. Rev. Lett. **95**, 016405 (2005).
[13] Y. X. Zhao and Z. D. Wang, Phys. Rev. Lett. **110**, 240404 (2013).
[14] A. P. Schnyder and P. M. R. Brydon, J. Phys. Condens. Matter **27**, 243201 (2015).
[15] B. Lian and S.-C. Zhang, Phys. Rev. B **94**, 041105 (2016).
[16] V. Mathai and G. C. Thiang, J. Phys. A **50**, 11LT01 (2017).
[17] V. Mathai and G. C. Thiang, arXiv:1611.08961.
[18] S. Sugawa, F. Salces-Carcoba, A. R. Perry, Y. Yue, and I. B. Spielman, arXiv:1610.06228.
[19] C. N. Yang, J. Math. Phys. **19**, 320 (1978).
[20] F. Wilczek and A. Zee, Phys. Rev. Lett. **52**, 2111 (1984).
[21] S.-C. Zhang and J. Hu, Science **294**, 823 (2001).
[22] A. Kitaev, in *Advances in Theoretical Physics: Landau Memorial Conference*, AIP Conf. Proc. No. 1134 (AIP, New York, 2009).
[23] S. Ryu, A. P. Schnyder, A. Furusaki, and A. W. W. Ludwig, New J. Phys. **12**, 065010 (2010).
[24] E. P. Wigner, Nachr. Akad. Wiss. Goettingen, Math. Phys. Kl. **31**, 546 (1932).
[25] F. J. Dyson, J. Math. Phys. **3**, 1199 (1962).
[26] H. Georgi and S. L. Glashow, Phys. Rev. Lett. **28**, 1494 (1972).